

See discussions, stats, and author profiles for this publication at: <https://www.researchgate.net/publication/231656442>

In Situ Scanning Tunneling Microscopy of Ordering Processes of Adsorbed Porphyrin on Iodine-Modified Ag(111)

ARTICLE *in* THE JOURNAL OF PHYSICAL CHEMISTRY · APRIL 1996

Impact Factor: 2.78 · DOI: 10.1021/jp953517j

CITATIONS

85

READS

15

4 AUTHORS, INCLUDING:



Masashi Kunitake

Kumamoto University

152 PUBLICATIONS 2,071 CITATIONS

SEE PROFILE



Kingo Itaya

Tohoku University

246 PUBLICATIONS 8,379 CITATIONS

SEE PROFILE

In Situ Scanning Tunneling Microscopy of Ordering Processes of Adsorbed Porphyrin on Iodine-Modified Ag(111)

Katsuhiko Ogaki, Nikola Batina, Masashi Kunitake, and Kingo Itaya^{*,†}

Itaya Electrochemistry Project, ERATO, JRDC, 2-1-1 Yagiyama-Minami, Taihaku-ku, Sendai 982, Japan

Received: November 28, 1995[®]

The iodine-modified Ag(111) substrate was employed as an electrode to investigate the adsorption of 5,10,15,20-tetrakis(*N*-methylpyridinium-4-yl)-21*H*,23*H*-porphine tetrakis(*p*-toluenesulfonate) (TMPyP) in an alkaline solution containing KI. It was found by using in situ scanning tunneling microscopy (STM) that water soluble TMPyP molecules were irreversibly adsorbed and formed highly ordered molecular adlayers on the surface of the iodine-modified Ag(111) electrode within the potential range of -0.35 to -0.10 V vs Ag/AgI. STM images revealed the characteristic shape, internal molecular structure, and molecular orientation of each TMPyP molecule in ordered adlayers. The ordered TMPyP adlayer usually consisted of stripes of several straight molecular rows with different orientations along the $\sqrt{3}$ direction of the underlying iodine adlayers. In each row, molecules were aligned with the same orientation. From the time-dependent imaging, the ordered molecular adlayer was found to grow in the specific $\sqrt{3}$ direction with an averaged growth rate of ca. 6 nm/s.

Introduction

It is almost completely established, at least in ultrahigh vacuum (UHV), that scanning tunneling microscopy (STM) can provide high-resolution images of organic molecules such as benzene,^{1,2} naphthalene,³ and copper phthalocyanine⁴ with their distinguishable molecular shapes and even internal structures.⁵ On the other hand, STM has also been recognized as an important in situ method for structural investigations of adsorbed adlayers on well-defined electrode surfaces in electrolyte solution with atomic resolution.⁶ Strongly adsorbed inorganic ions such as halides,^{7–10} cyanide,^{11,12} and sulfate/bisulfate¹³ are known to form ordered adlayers, and their structures have been determined directly by in situ STM with atomic resolution. Although such rather small inorganic species adsorbed on the electrode surface can be relatively easily visualized by in situ STM,^{6–13} not many in situ STM images comparable to those achieved in UHV have been reported for organic molecules adsorbed at the electrode–electrolyte interface with high resolution.

The adsorption of organic molecules on electrode surfaces in electrolyte solutions is an important subject in electrochemistry for elucidating the role of adsorbed molecules in various electrochemical reactions.^{14–16} A few recent papers reported in situ STM images with relatively high-resolution for ordered adlayers of DNA bases such as cytosine¹⁷ and, more recently, xanthine¹⁸ adsorbed on highly ordered pyrolytic graphite (HOPG) as well as on Au(111). Although HOPG and similar layered crystals such as MoS₂ have been almost exclusively used as the substrate for the study of molecules,⁵ it is known that these substrates exhibited large corrugation amplitudes, 0.05–0.2 nm, for the individual carbon and sulfur atoms in STM images, which sometimes interfered with the observation of small corrugations associated with adsorbed organic molecules.¹⁹

It had long been desired by us to find a more appropriate substrate to investigate adsorbed organic molecules in electrolyte solutions, and we recently discovered a novel substrate with great generality on which molecules such as porphyrine and crystal violet were found to form highly ordered adlayers. The

substrate was an iodine monolayer adsorbed on the Au(111) surface, the so-called iodine-modified Au.^{19–21} The internal molecular structures, orientations, and packing arrangements of these molecular adlayers were visualized in solutions by in situ STM with surprisingly high resolution.^{19–21} It was briefly discussed in our previous paper¹⁹ that relatively weak van der Waals type interactions between the hydrophobic iodine adlayer and the organic molecules should be a key factor to promote self-ordering processes involving the surface diffusion of molecules on the iodine-modified Au(111).

The iodine adlayers have intensively been investigated on various single crystal electrodes such as Au, Ag, Pt, Rh, and Pd using ex situ LEED (low-energy electron diffraction),^{15,16} in situ STM^{7–9,22,23} and in situ surface X-ray scattering.²⁴ The iodine adlayers on these substrates can be thought to be composed of neutral atoms rather than negatively charged iodide ions, providing the hydrophobic property.^{15,16} Therefore, it is our great interest to investigate the adsorption of organic molecules on other iodine-modified electrodes in order to evaluate the role of the iodine adlayer in the self-ordering process. The iodine-modified Ag(111) electrode should be one of the most interesting substrates because the structures of the iodine adlayer on Ag was previously well characterized^{15,25} and also because the bare Ag electrode has frequently been used as the electrode for the adsorption of organic molecules.¹⁴ In this paper, we report our successful in situ STM imaging of a highly ordered adlayer of 5,10,15,20-tetrakis(*N*-methylpyridinium-4-yl)-21*H*,23*H*-porphine tetrakis(*p*-toluenesulfonate) (TMPyP) on Ag(111) in an alkaline electrolyte solution in the presence of KI (0.1 mM KI + 10 mM KF + 0.1 mM KOH at pH = 10). This buffered KI solution was previously used for the ex situ LEED study of the iodine adlayer on Ag(111).²⁵ In situ STM with near-atomic resolution allowed us to determine molecular orientations and packing arrangements of TMPyP. Time-sequenced STM images were acquired to evaluate the self-ordering process, indicating that the ordered monolayer of TMPyP grows in specific $\sqrt{3}$ directions with respect to Ag(111).

Experimental Section

The experimental details for in situ STM have been described elsewhere.^{9,13} A Nanoscope III (Digital Instruments, USA) with

[†] Department of Applied Chemistry, Faculty of Engineering, Tohoku University, Aoba-ku, Sendai 980, Japan.

[®] Abstract published in *Advance ACS Abstracts*, April 1, 1996.

our laboratory-designed electrochemical cell was used. All images have been acquired in a constant current mode by using electrochemically etched tungsten or commercial Pt–Ir (80:20) wires. Side walls of the tunneling tips were isolated from the electrolyte solution by coating an insulating material such as glass, nail enamel, or a Teflon polymer (Daikin Co. Tokyo). Because of the possibility of contamination from the coating, we employed three different tips for the purpose of comparison: glass-coated Pt–Ir, Teflon polymer-coated W, and nail enamel-coated W. All tips were previously soaked in the electrolyte solution for several hours to eliminate soluble contaminants before starting STM measurements. Essentially, no difference was found for the structure of the TMPyP adlayer using the above-mentioned tips. Because of the simplicity of preparation and handling during the experiment, the nail enamel-coated W tips were mainly used in the present study. Ag/AgI and platinum were used as the reference and counterelectrodes, respectively. All electrode potentials are reported with respect to the reversible Ag/AgI reference electrode. Experiments were carried out in 0.1 mM KI bufferd with 10 mM KF + 0.1 mM KOH at pH = 10, which was previously used by Salaita et al.²⁵ for their investigation of the structure of the iodine adlayer on Ag(111) by *ex situ* LEED.

It was confirmed in our previous²⁶ and present papers that Ag films (more than 50 layers) deposited electrochemically on a well-defined Au(111) surface in a 1 mM AgClO₄ + 0.1 M HClO₄ solution could be used as an ideal Ag(111) electrode. In situ STM as well as LEED and Auger electron spectroscopy (AES) indicated that the Ag film was a well-ordered and pure Ag(111). No signal of Au was detected by AES. The deposition was carried out on a flame-annealed Au(111) in the solution at –0.1 V vs. a Ag/Ag⁺ reference electrode.²⁶ After the deposition of ca. 50 Ag monolayers, the electrode was rinsed with pure water and transferred into an electrochemical cell containing the buffered KI solution. During the transfer, the Ag(111) surface was protected from contamination by a droplet of pure water. The contact between the electrode and the electrolyte solution was accomplished under potential control at about –0.15 V vs. Ag/AgI in order to avoid bulk formation of AgI which was found to occur at open circuit. The structure of the iodine adlayer was determined by in situ STM. After the examination of the iodine adlayer, an aqueous solution of TMPyP (Doujin Co., Japan) was injected into the buffered KI solution. TMPyP concentrations used were typically 10^{–7} to 10^{–6} M.

KI (special grade), KOH (ultrapure grade), KF (suprapure grade), AgClO₄ (special grade) were supplied from Kanto Chemical Co., Japan.

Results and Discussion

Voltammetry. Figure 1a shows a cyclic voltammogram (CV) obtained on an Ag(111) film deposited on Au(111) in the buffered KI solution at pH = 10 in the absence of TMPyP. Two cathodic peaks at –0.65 and –0.7 V in the negative potential range are partially due to reductive desorption of the adsorbed iodine on Ag(111). The anodic peaks corresponding the readsorption of iodide appear at almost the same potentials. The anodic current (I) that is steeply increased at ca. 0 V is due to the bulk formation of AgI, and the corresponding cathodic peak is due to the reduction of the bulk AgI to form metallic Ag. Note that a small reversible peak (II) can be clearly seen at potentials slightly negative than 0 V. The potential and current of each of these peaks are in good agreement with those reported for the same solution at a bulk single crystal of Ag(111) by Salaita et al.²⁵ This agreement indicates that the Ag

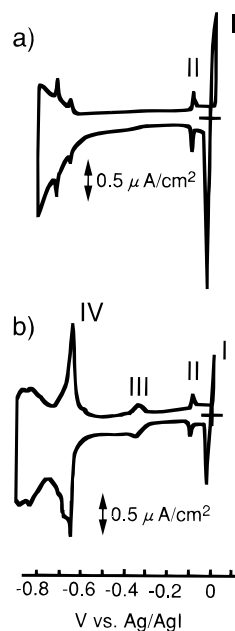


Figure 1. Cyclic voltammograms of iodine-modified Ag(111) recorded in 0.1 mM KI + 10 mM KF + 0.1 mM KOH (pH = 10) in the absence (a) and presence (b) of 2×10^{-7} M TMPyP. The scan rate of the electrode potential was 5 mV/s.

film used in this study was a well-defined (111) surface. Salaita et al. reported LEED patterns of $(\sqrt{3} \times \sqrt{3})R30^\circ$ with a triangular splitting at negative potentials between –0.3 V vs a Ag/AgCl reference electrode and the hydrogen limit.²⁵ A structural transition from triangular to hexagonal splitting in the LEED pattern was also reported to occur near the peak potential (II). However, we recently conducted a more detailed study of the structural change of the iodine adlayer on Ag(111) and found a continuous compression of the iodine adlattice from square to $(\sqrt{3} \times \sqrt{3})R30^\circ$ at more positive potentials in the negative potential window with respect to peak II. The $(\sqrt{3} \times \sqrt{3})$ - $R30^\circ$ pattern with no splitting was found to appear at the negative end of the peak II potential region. At the positive end of peak II, a rotated hexagonal adlattice was found to appear with an additional Moiré pattern that was similar to that found for the iodine on Au(111) as described in our previous paper.⁹ A detailed study will be described in a separate paper.²⁷

Figure 1b shows a CV obtained in the same electrolyte in the presence of 2×10^{-7} M TMPyP. The electrode potential, prior to scanning the potential, was held at –0.15 V for more than 30 min in order to establish an equilibrium state. Although peaks I and II in Figure 1b are very similar to those found in the pure electrolyte solution as shown in Figure 1a, two new sets of peaks appear clearly at –0.35 V (III) and –0.65 V (IV), respectively, in the solution containing TMPyP. The relatively large peak IV may still be due to partial adsorption–desorption of the iodine, which may be affected by the presence of the TMPyP adlayer on top of the iodine monolayer. The desorption of the adsorbed TMPyP does not appear to take place in the potential range of Figure 1b. All peaks were found to be highly reversible even at high scan rates. If the adsorbed TMPyP molecules were desorbed from the electrode surface during the partial desorption of the iodine adlayer, it should take a longer period of time for the readsorption of TMPyP at the presently used concentration of 2×10^{-7} M, which should result in the appearance of irreversible anodic peaks in the positive going scan. The rather small peak at –0.35 V is thought to be due to a structural transition involving the organic adlayer, which will be discussed later.

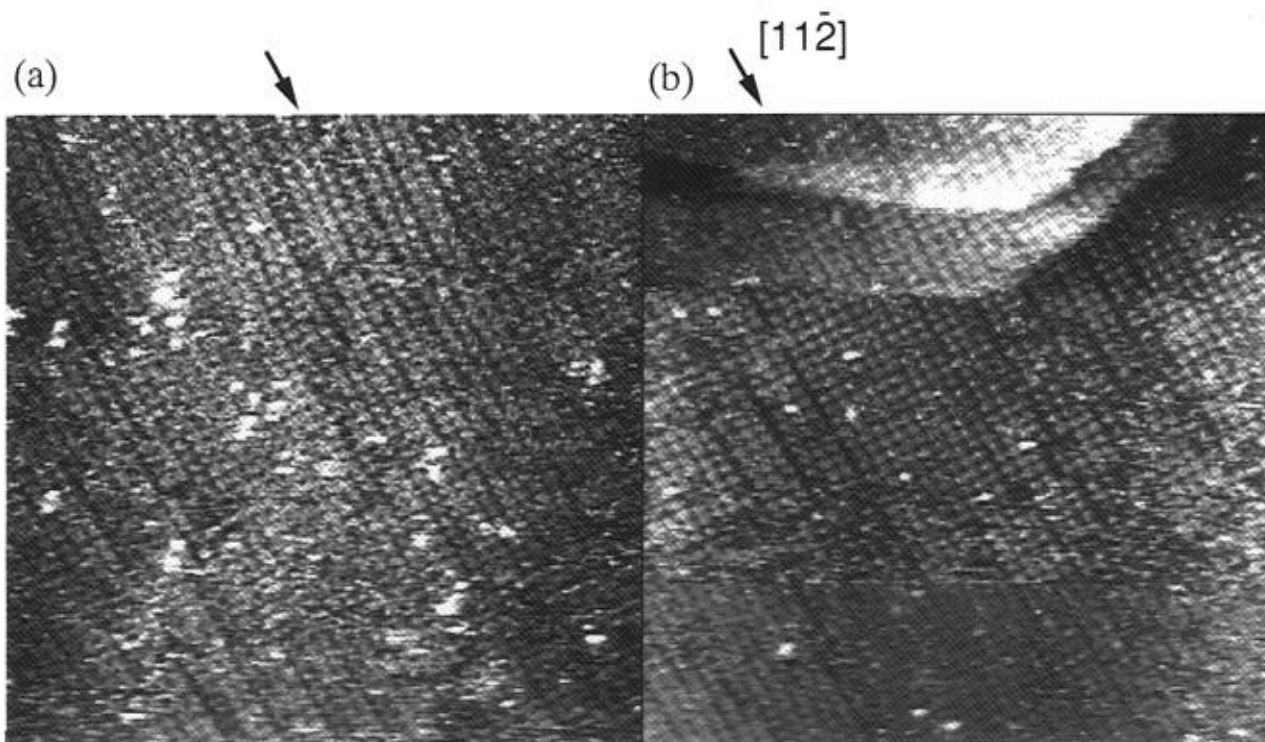


Figure 2. In situ STM images ($50 \times 50 \text{ nm}^2$) of ordered TMPyP molecular arrays formed on iodine-modified Ag(111) surfaces on (a) an atomically flat terrace and (b) three terraces separated with monoatomic steps. TMPyP molecular rows are aligned along the $[11\bar{2}]$ direction, marked by an arrow. Images were recorded in buffered KI solution in the presence of $2 \times 10^{-7} \text{ M}$ TMPyP at -0.15 V vs Ag/AgI. The tunneling current is 0.5 nA ; tip potential is 0.015 V .

In Situ STM. As described above, in situ STM revealed a $(\sqrt{3} \times \sqrt{3})R30^\circ$ structure for the iodine adlayer at -0.15 V before the injection of TMPyP. After the addition of TMPyP, STM images for the iodine adlayer usually became unclear within the first 15 min because of the adsorption of TMPyP, and then ordered adlayers became visible, extending over the atomically flat terraces. However, it was found in this study that the adsorbed TMPyP molecules on the iodine-modified Ag(111) formed ordered structures only in the rather narrow potential range between the voltammetric peaks marked II and III in Figure 1b.

Figure 2 shows two typical STM images acquired in relatively large areas of $50 \times 50 \text{ nm}^2$ at -0.15 V . The images were acquired intentionally on an atomically flat terrace (a) and on an area showing monoatomic steps (b), respectively. It was surprising that individual molecules with a square shape were discernable in such large areas. Clearly, the iodine-modified Ag(111) surface was almost completely covered by the adsorbed molecules. Note also that individual TMPyP molecules existed on both upper and lower terraces in close proximity to monoatomic steps. However, it was always noticed that appreciable numbers of phase boundaries appeared as depressed lines along the $[11\bar{2}]$ direction or the $\sqrt{3}$ direction. Despite the appearance of such boundaries along the $\sqrt{3}$ direction, the STM images clearly revealed that the TMPyP molecular rows formed more regularly with a long-range ordering along the $\sqrt{3}$ direction. These molecular rows appeared as straight lines along the $\sqrt{3}$ direction, extending over the terraces. An intermolecular distance was found to be $\text{ca. } 1.7 \pm 0.1 \text{ nm}$ in these rows. Note that straight molecular rows were also found on the upper terraces along the same $\sqrt{3}$ direction as shown in Figure 2b. In addition, it is also clear that TMPyP formed almost square adlattices in ordered domains, indicating that an ordering process was also involved in the $[110]$ direction, which is perpendicular to the $\sqrt{3}$ direction. However, it is of interest to note that the molecular rows along the $[110]$ direction appear to be organized

by a rather small number of molecules. For example, sets of two or three molecular rows along the $[110]$ direction separated by the phase boundary described above were frequently observed. These sets of molecular rows are more clearly seen on the lowest terrace in the image shown in Figure 2b.

Figure 3a shows a high-resolution STM image acquired in an area of $24 \times 24 \text{ nm}^2$, revealing more clearly internal molecular structures and molecular orientations in the ordered adlayer. The STM image included the TMPyP arrays formed on two adjacent terraces separated by a monoatomic step. An individual TMPyP molecule can be clearly recognized as a square with four additional bright spots at the corners. As described in our recent paper,¹⁹ these bright spots can be attributed to the pyridinium units in the chemical structure shown in Figure 3b. The molecules along the $[11\bar{2}]$ direction can be seen to align with the same orientation, resulting in the straight lines as shown in Figure 2. However, domains with the same molecular orientation are rather narrow, forming long stripes along the $[11\bar{2}]$ direction. On the lower terrace, at the right-hand side of the image, striped domains, consisting of three molecular rows, can be seen. Although all molecules in each domain show the same orientation, the molecules in the adjacent domains were rotated by $\text{ca. } 45^\circ$ with respect to those in the central domain. The structure of the TMPyP adlayer observed on this lower terrace can be illustrated by the model shown in Figure 4. The model represents three adjacent domains (A, B, A) in the TMPyP adlayer separated by domain boundaries indicated by the solid lines. It is clear that the molecules are not uniformly aligned along the $[110]$ direction but form zig-zag patterns. In the domains denoted by A, the adsorbed molecules form an almost square lattice. On the other hand, a slightly tilted lattice is formed in domain B.

The structure of TMPyP on the iodine-modified Ag(111) is clearly different from that found on the iodine-modified Au(111) in a HClO_4 solution as described previously.¹⁹ On the iodine-modified Au(111), every TMPyP molecule possessed the

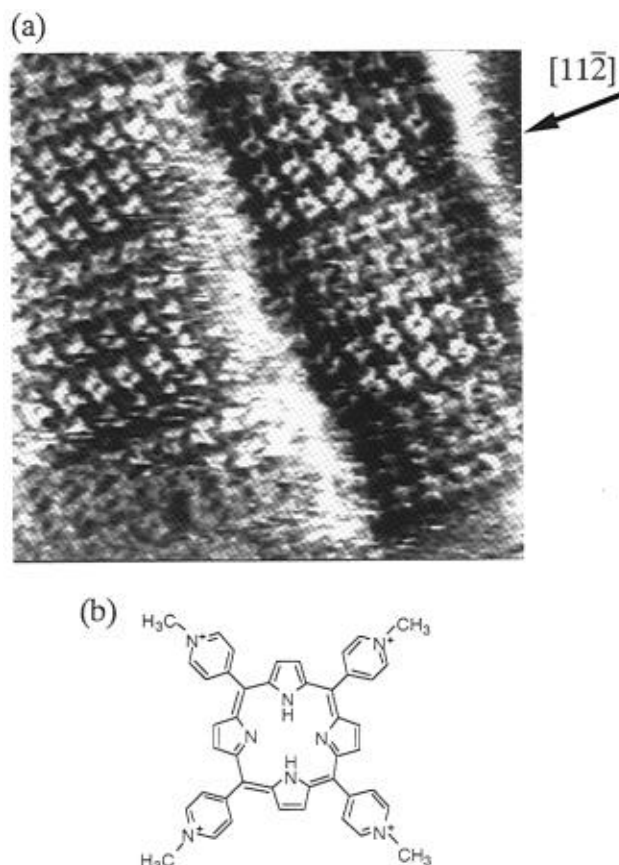


Figure 3. High-resolution in situ STM image ($24 \times 24 \text{ nm}^2$) of TMPyP array (a). The image was recorded under the same experimental conditions as for Figure 2. The chemical structure of TMPyP is shown in (b).

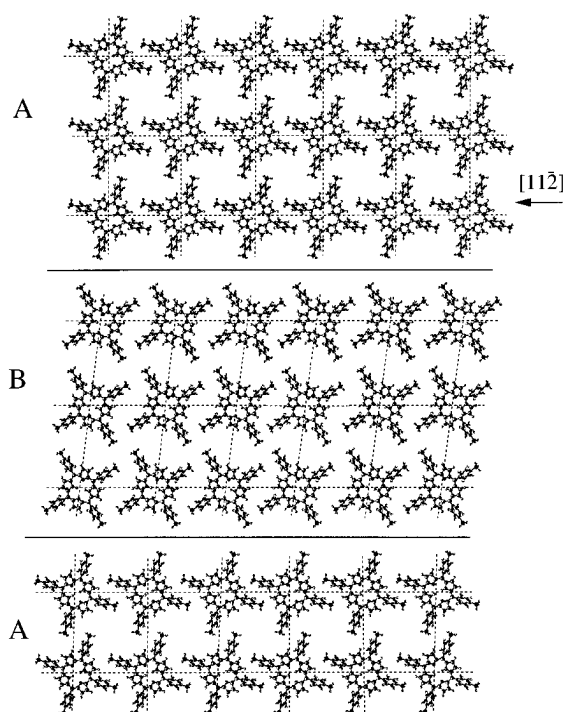


Figure 4. Schematic representation of the TMPyP array structure with three domains noted as A, B, and A.

same molecular orientation along a specific direction, as was found presently along the $[11\bar{2}]$ direction. However, a rotation angle of 45° was found between neighboring molecules in a different direction on the Au substrate (see Figure 3 in ref 19). In general, many factors should be taken into account to explain

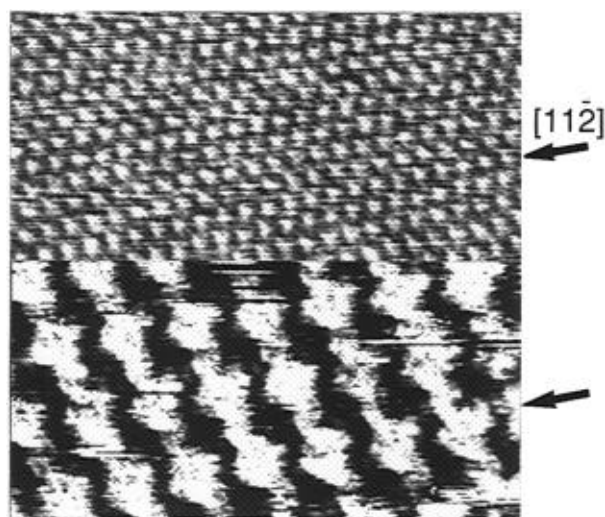


Figure 5. Two superimposed images ($11.4 \times 11.4 \text{ nm}^2$) acquired at different tunneling currents. The upper and the lower halves of the image were obtained at 50 and 1.5 nA, respectively. One of the molecular rows is parallel to the $[11\bar{2}]$ direction (marked by arrow). Other experimental conditions were the same as for Figure 2.

the adlayer structures and the difference between those on different substrates. The interactions between the adsorbed molecules and the iodine adlayers should be different on Ag and Au. However, we believe that the architecture of TMPyP is primarily determined by the structure of the underlying iodine adlayer. In the buffered KI solution at $\text{pH} = 10$, we observed by in situ STM and ex situ LEED a continuously varying series of adlayers from a square ($\sqrt{3} \times \sqrt{3}R-30^\circ$) structure at -0.35 V to a triangular ($\sqrt{3} \times \sqrt{3}R30^\circ$) structure at -0.13 V . It was also found that one of three equivalent $\sqrt{3}$ directions was always unchanged between the above two potentials.²⁷ Presumably, the molecules align in this particular $\sqrt{3}$ direction. Figure 5 shows a superimposed image consisting of two images acquired consecutively at different tunneling currents. The upper and lower parts of the image were obtained at 50 and 1.5 nA, respectively. As described previously,¹⁹ the iodine adlayer was made visible through the organic layer by increasing the tunneling current. It was found in this study that the STM image of iodine atoms underlying the TMPyP layer exhibited a distortion from the perfect ($\sqrt{3} \times \sqrt{3}R30^\circ$) structure with 3-fold symmetry. Note that the straight TMPyP rows indicated by the arrow signs in Figure 5 are indeed parallel to one of the atomic rows of iodine, along the $[11\bar{2}]$ direction. This result also supports our assumption that the long molecular chains with the same orientation were formed along the invariable $\sqrt{3}$ direction in the iodine adlayer. However, it must be noted that the structure of TMPyP did not show potential dependence in the range between the peaks of II and III in Figure 1b. The images shown in Figures 2 and 3 were consistently observed in this potential range, suggesting that the structure of the iodine adlayer underneath the TMPyP layer also has a defined structure. However, the ordered molecular array abruptly disappeared when the electrode potential was made more negative than that of peak III, suggesting that peak III is due to a phase transition between the ordered and disordered phases. Figure 6 shows an example of a composite-domain image, obtained by changing the electrode potential. The upper and lower parts of the image were acquired at -0.15 and -0.4 V , respectively. It is clear that the individual TMPyP molecule disappeared in the lower part of the image. Also, it is interesting to note that the lower part of the image obtained at a tunneling current of 1 nA shows no atomically resolved structure of TMPyP or that of iodine. This result strongly suggests that TMPyP molecules with a relatively large mobility mask the corrugation of the underlying

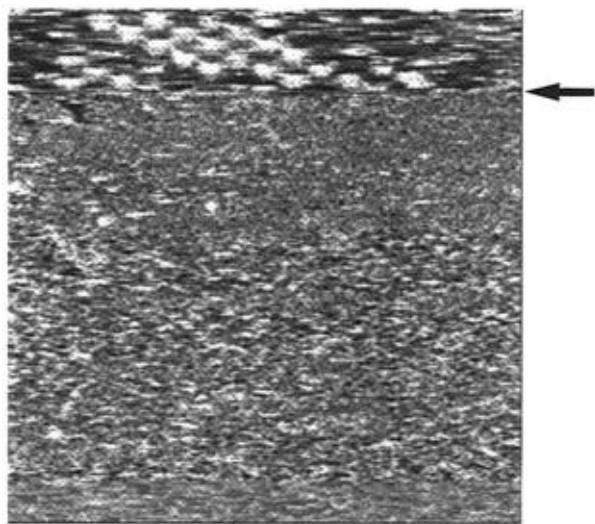


Figure 6. Composite image ($22 \times 22 \text{ nm}^2$) acquired upon stepping the potential from -0.15 to -0.4 V (lower part of the image). The potential was stepped at the position marked by an arrow. Tunneling current is 1 nA ; tip potential is 0.02 V .

iodine adlayer. A similar result was previously found for the underpotential deposition of Cu on Au(111).²⁸ Note that an ordered adlayer of TMPyP reappeared in a few minutes after the electrode potential was stepped back to -0.15 V , indicating that the phase transition involved in peak III was quite reversible. The above result clearly indicated that in situ STM could be applied to determine structural changes in molecular adlayers due to the phase transition. Indeed, Cunhan and Tao recently demonstrated that an order-disorder transition in a 2,2'-bipyridine monolayer on Au(111) was successfully followed by in situ STM in a NaClO_4 solution.²⁹ And various cytosine adlayers were found to form on Au(111), depending on the electrode potential.³⁰

In situ STM also allowed us to investigate the dynamics of the formation of the ordered TMPyP adlayer on the iodine-modified Ag(111) surface. To obtain STM images showing an intermediate state was not easy because of the fairly rapid formation of the ordered domains under the conditions where the nucleation of the ordered domain was already started. The

two images shown in Figure 7 were successfully recorded during a short time interval of 64 s , just a few minutes after the addition of TMPyP in the electrolyte solution. Each image was acquired in 32 s . The image shown in Figure 7a revealed that the surface was dominantly covered by a disordered adlayer of TMPyP (shown on the left-hand side of the image). However, ordered domains can also be seen on the right-hand portion of the image. The blurred appearance of the individual molecules at the boundaries as well as in the middle of the ordered domain suggests that TMPyP molecules still have freedom to move in the layer, particularly near the boundaries. Nevertheless, it was interesting to observe that the ordered domain of the TMPyP adlayer increased in area significantly after 32 s and expanded in the $[11\bar{2}]$ direction, forming straight molecular chains as described above. Using a surface defect found at the lower-left portion of the images as a land-marker, we estimated an average growth rate of ca. 6 nm/s for molecular rows along the $[11\bar{2}]$ direction. This growth rate shows that, under the present experimental conditions, about four TMPyP molecules were incorporated per second into the ordered domain. The results shown in Figure 7 support our vision of the role of the iodine adlayer during the formation of well-ordered molecular arrays on the iodine-modified single crystal metal electrodes via self-organization processes. Relatively weak van der Waals type interactions between the organic molecules and the iodine adlayer on top of the metal substrate allow the randomly adsorbed molecules to diffuse on the iodine adlayer, resulting in self-organization of the adsorbed molecules and establishment of an ordered molecular phase.

Finally, it is noteworthy that we have examined the adsorption of various organic molecules with different shapes such as crystal violet, triangular, and linear conjugated molecules on the iodine-modified Ag and Au^{20,21} and found that those molecules also formed highly ordered adlayers. The iodine adlayers formed on different single crystal electrodes such as Pt and Rh are also of special interest in evaluating the role of the iodine adlayer in the self-organization processes.³¹ Such knowledge is expected to provide a key to the full understanding of the role of iodine adlayers in the formation of ordered phases of adsorbed molecules.

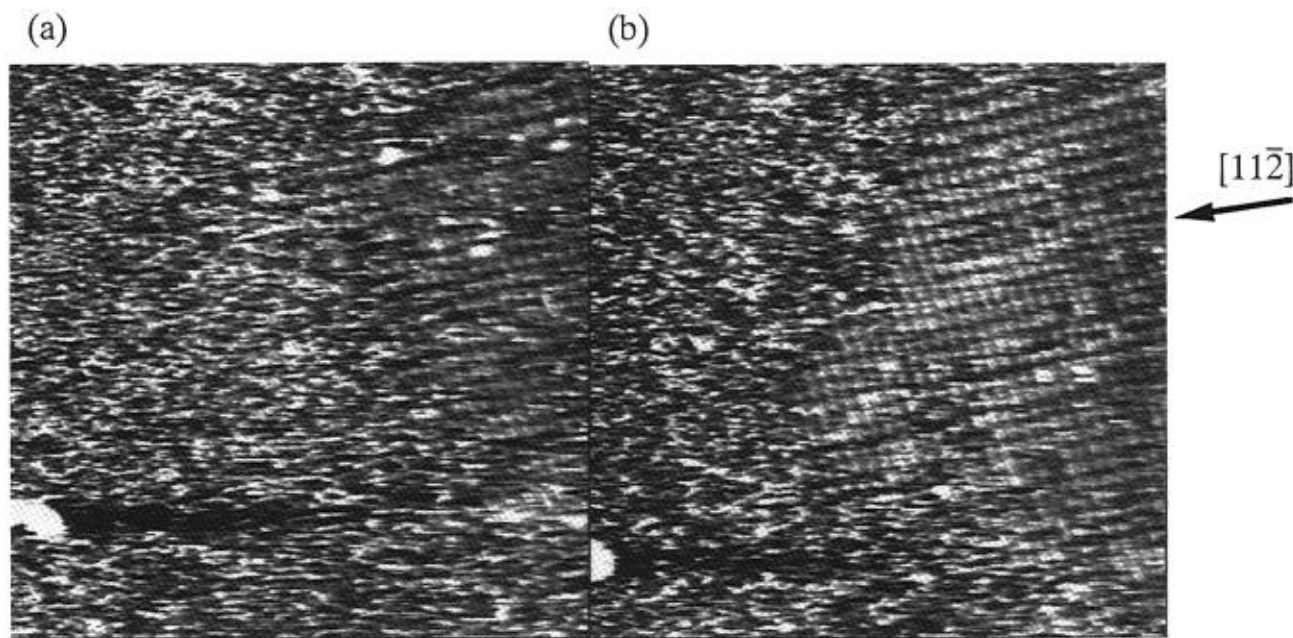


Figure 7. Two consecutively recorded images ($50 \times 50 \text{ nm}^2$) acquired at an early stage of the TMPyP array formation at -0.15 V . Each image was obtained in 32 s . Tunneling current is 1 nA ; tip potential is 0.02 V .

Conclusions

Following our previous suggestion¹⁹ that iodine-modified single crystal electrode surfaces can be a unique medium for the preparation and growth of highly ordered molecular adlayers, we studied the formation of the TMPyP ordered adlayer on the iodine-modified Ag (111) from an alkaline solution containing KI. The results of our present study clearly show that water-soluble TMPyP molecules easily adsorb and form an ordered layer on the surface of the iodine-modified Ag (111) electrode within the potential range -0.35 to -0.10 V vs Ag/AgI. In order to characterize the structure of the ordered molecular layer and to define the ordering process of the adsorbed molecules, in situ STM was employed. It allowed visualization of the adsorbed layer directly at the electrode–electrolyte interface, revealing details such as the shape of individual molecules with internal molecular structure and molecular orientation. On the basis of the STM examination, it was found that the electrode surface was completely covered by an ordered TMPyP adlayer consisting of stripes of several, usually three, rows of molecules. The stripes as well as the molecular rows were always found to be aligned along the $\sqrt{3}$ direction of the iodine adlattice. Although the molecular orientation was different between the stripes, within a single molecular row all molecules were oriented in the same direction. The ordering process of the molecular layer was controlled by the underlying iodine adlayer. Shifting the electrode potential out of the above-mentioned potential window resulted in the disordering of the molecular layer and the disappearance of the STM images. A series of consecutively recorded STM images revealed the early stages of the growth of the molecular layer to be in a preferential $\sqrt{3}$ direction, and the average growth rate of the molecular adlayer was estimated to be 6 nm/s. Finally, it is worthwhile to mention that the in situ STM findings were in perfect harmony with the electrochemical data and the present knowledge about the structure of the iodine adlayer on the Ag (111) surface.

Acknowledgment. This work was supported by ERATO-Itaya Electrochemiscopy Project, ERATO/JRDC. We are grateful to Dr. Y. Okinaka for his help in the writing of this manuscript. We thank Professor S. M. Lindsay (Arizona State University) for sending us the paper³⁰ prior to its publication.

References and Notes

- (1) Ohtani, H.; Wilson, R. J.; Chiang, S.; Mate, C. M. *Phys. Rev. Lett.* **1988**, *60*, 2398.
- (2) Weiss, P. S.; Eigler, D. M. *Phys. Rev. Lett.* **1993**, *71*, 3139.
- (3) Hallmark, V. M.; Chiang, S.; Brown, J. K.; Woll, Ch. *Phys. Rev. Lett.* **1991**, *66*, 48.
- (4) Lippel, P. H.; Wilson, R. J.; Miller, M. D.; Woll, C.; Chiang, S. *Phys. Rev. Lett.* **1989**, *62*, 171.
- (5) Rabe, J. P. *Ultramicroscopy* **1992**, *42–44*, 41, and references cited therein.
- (6) Siegenthaler, H. *Scanning Tunneling Microscopy II*; Wiesendanger, R., Guntherodt, H.-J., Eds.; Springer-Verlag: Berlin, 1992; p 7.
- (7) Yau, S.-L.; Vitus, C. M.; Schardt, B. C. *J. Am. Chem. Soc.* **1990**, *112*, 3677.
- (8) Gao, X.; Weaver, M. J. *J. Am. Chem. Soc.* **1992**, *114*, 8544.
- (9) Yamada, T.; Batina, N.; Itaya, K. *J. Phys. Chem.* **1995**, *99*, 8817, and references cited therein.
- (10) Suggs, D. W.; Bard, A. J. *J. Am. Chem. Soc.* **1994**, *116*, 10725.
- (11) McCarley, R. L.; Bard, A. J. *J. Phys. Chem.* **1992**, *96*, 7410.
- (12) Stuhlmann, C.; Villegas, I.; Weaver, M. J. *Chem. Phys. Lett.* **1994**, *219*, 319.
- (13) Wan, L.-J.; Yau, S.-L.; Itaya, K. *J. Phys. Chem.* **1995**, *99*, 9507, and references cited therein.
- (14) Lipkowsky, J.; Ross, P. N., Eds. *Adsorption of Molecules at Metal Electrodes*; VCH Publishers: New York, 1992.
- (15) Hubbard, A. T. *Chem. Rev.* **1988**, *88*, 633.
- (16) Soriaga, M. P. *Prog. Surf. Sci.* **1992**, *39*, 325.
- (17) Tao, N. J.; DeRose, J. A.; Lindsay, S. M. *J. Phys. Chem.* **1993**, *97*, 910.
- (18) Tao, N. J.; Shi, Z. *J. Phys. Chem.* **1994**, *98*, 1464.
- (19) Kunitake, M.; Batina, N.; Itaya, K. *Langmuir* **1995**, *11*, 2337.
- (20) Batina, N.; Kunitake, M.; Itaya, K. *J. Electroanal. Chem.*, in press.
- (21) Batina, N.; Kunitake, M.; Itaya, K. *Extended Abstracts*, 188th ECS Meeting, Chicago, Illinois, October 8–13, 1995; Vol. 95-2, pp 1425–1427.
- (22) Sugita, S.; Abe, T.; Itaya, K. *J. Phys. Chem.* **1993**, *97*, 8780.
- (23) Batina, N.; Yamada, T.; Itaya, K. *Langmuir* **1995**, *11*, 4568.
- (24) Ocko, B. M.; Watson, G. M.; Wang, J. *J. Phys. Chem.* **1994**, *98*, 897.
- (25) Salaita, G. N.; Lu, F.; Laguren-Davidson, L.; Hubbard, A. T. *J. Electroanal. Chem.* **1987**, *229*, 1.
- (26) Ogaki, K.; Itaya, K. *Electrochim. Acta* **1995**, *40*, 1249.
- (27) Ogaki, K.; Yamada, T.; Okubo, S.; Itaya, K. In preparation.
- (28) Hachiya, T.; Honbo, H.; Itaya, K. *J. Electroanal. Chem.* **1991**, *315*, 265.
- (29) Cunha, F.; Tao, N. J. *Phys. Rev. Lett.* **1995**, *75*, 2376.
- (30) Wandlowski, Th.; Lampner, D.; Lindsay, S. M. *J. Electroanal. Chem.*, in press.
- (31) Batina, N.; Kunitake, M.; Kim, Y.-G.; Ogaki, K.; Wan, L.-J.; Itaya, K. In preparation.

JP953517J